Carbohydrate Polymers 238 (2020) 116182

Contents lists available at ScienceDirect

Carbohydrate Polymers

journal homepage: www.elsevier.com/locate/carbpol

In situ generated silica reinforced polyvinyl alcohol/liquefied chitin biodegradable films for food packaging

Jie Zhang[a,b], Wen-Rong Xu[a,*], Yu-Cang Zhang[a,*], Xu-Dong Han[a], Chen Chen[b], Ao Chen[b]

[a] Key Laboratory of Advanced Materials of Tropical Island Resources of Ministry of Education, Hainan Provincial Key Laboratory of Fine Chemistry, School of Chemical Engineering and Technology or School of Science, Hainan University, Haikou, 570228, PR China
[b] Hainan Health Management College, Haikou, 570228, PR China

ARTICLE INFO

Chemical compounds studied in this article:
Polyethylene glycol (PubChem CID: 174)
Glycerin (PubChem CID: 753)
Polyvinyl alcohol (PubChem CID: 11199)
Ethanol (PubChem CID: 702)
Sulfuric acid (PubChem CID: 1118)
KBr (PubChem CID: 253877)
Na_2SiO_3 (PubChem CID: 23266)

Keywords:
Chitin
Liquefaction
Polyvinyl alcohol
Silica
Biodegradable film

ABSTRACT

In previous report, polyvinyl alcohol/liquefied ball-milled chitin (PVA/LBMC) blend films with good antibacterial activity were successfully prepared. To further develop a biodegradable food packaging material, various amounts of nano-silica were introduced in situ by the hydrolysis of Na_2SiO_3 to give a series of silica-reinforced PVA/LBMC blend films. Their structure, morphology, mechanical and thermal properties, food preservation and degradation behavior in soil were comprehensively characterized. The results showed that when the content of Na_2SiO_3 was 0.2 wt %, the blend film 4PVA-LBMC-0.2Si displayed the optimized performance. Its tensile strength, and the maximum weight loss rate temperature reached 51 MPa and 307 °C, respectively, which were significantly improved than those of silica-free film. The preservation tests of cherries showed its good fresh keeping performance. Although the degradation rate of silica-reinforced blend films in the soil was slightly decreased, it remained at a good level of 43 % after 30 days of burial.

1. Introduction

Petroleum-based plastics, such as polystyrene (Li, Ni, & Zeng, 2017), polypropylene (Felix & Gatenholm, 2010) and polyvinyl chloride (Song, Wei, Wang, & Zhang, 2017), are widely used as food packaging materials due to their great combination of strength, stability, transparency, permeability and flexibility. However, their nondegradable nature inevitably leads to environmental problems, coupled with the gradual depletion of petroleum, promoting the rapid development of biodegradable bioplastics research (He et al., 2017). According to the European Bioplastics organization, bioplastic is defined as the renewable resource-based plastics or the biodegradable plastics (Peelman et al., 2013). Among the various renewable sources of bioplastics, chitin biomass, as well as its alkaline deacetylated derivative chitosan (CS), is particular attractive due to their abundant reserves, biodegradability, film formability, nontoxicity, biocompatibility and antibacterial activity (He et al., 2014; Kittle et al., 2012; Wang, Li, & Li, 2016). Encouragingly, chitin/chitosan based films have found applications in numerous fields, such as food packaging (Broek, Knoop, Kappen, & Boeriu, 2015; Siripatrawan & Noipha, 2012), wound dressing (Alminderej & El-Ghoul, 2019; Jayakumar, Prabaharan, Kumar, Nair, & Tamura, 2011) and water treatment (Vakili et al., 2014; Yan et al., 2019). Nonetheless, the poor solubility of chitin and chitosan in water and common organic solvents is a major limitation for their better utilization. As reported, their solubility is greatly affected by molecular weight, surrounding pH conditions and degree of deacetylation (Aye, Karuppuswamy, Ahamed, & Stevens, 2006). Generally, lower molecular weight, higher degree of deacetylation and lower pH are favorable for their solubility (Goy, Britto, & Assis, 2009). It is well known that chitosan can be dissolved in a dilute acidic aqueous solution below pH 6.5 because the protonation of its free active amino group affords a soluble form of its glucosamine unit, $R\text{-}NH_3^+$ (Aider, Arul, Mateescu, Brunet, & Bazinet, 2006; Kumar, Muzzarelli, Muzzarelli, Sashiwa, & Domb, 2004). Besides, chitosan exhibits its antibacterial activity only in an acidic medium, which is mainly attributed to the improvement of solubility (Mural, Kumar, Madras, & Bose, 2016; Rabea, Badawy, Stevens, Smagghe, & Steurbaut, 2003; Tang et al., 2010). In addition to the solubility issue of chitin and chitosan, films made with only

* Corresponding authors.
E-mail addresses: xuwr2016@hainanu.edu.cn (W.-R. Xu), yczhang@hainanu.edu.cn (Y.-C. Zhang).

https://doi.org/10.1016/j.carbpol.2020.116182
Received 4 January 2020; Received in revised form 13 March 2020; Accepted 14 March 2020
Available online 18 March 2020

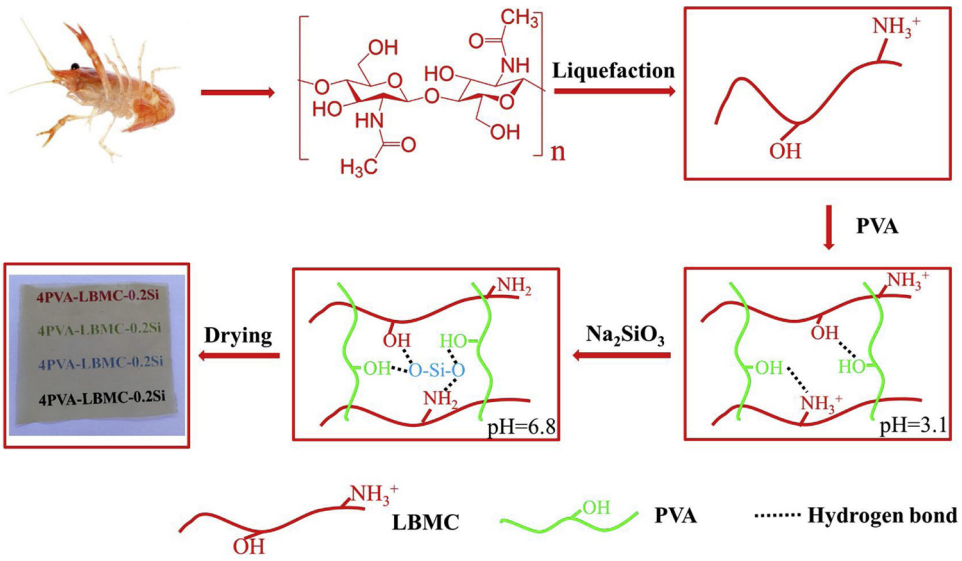

Fig. 1. Schematic diagram of silica reinforced PVA/LBMC biodegradable films preparation.

chitosan also suffer problems of unsatisfactory mechanical properties and poor water resistance (Wang et al., 2005; Xu, Ren, & Hanna, 2010). Blending as an effective method to modify the polymer properties has been extensively applied to impart new properties to chitosan films. Polyvinyl alcohol (PVA) is a biocompatible, non-toxic and chemical resistant polymer that is extensively used in blend films (Ifuku et al., 2013; Peresin, Habibi, Zoppe, Pawlak, & Rojas, 2010) and food packaging (Liu, Xu, Zhao, Liu, & Li, 2017). It has been reported that blending chitosan with polyvinyl alcohol (PVA) can significantly enhance the mechanical and thermal properties of the blend films (Tripathi, Mehrotra, & Dutta, 2009). Moreover, the introduction of nanofillers such as cellulose nanofibers (Koga, Nagashima, Huang, Zhang, & Yanagida, 2019), silver nanoparticles (Abdelgawad, Hudson, & Rojas, 2014) and nano-silica (Li et al., 2018) also contributes to improving the properties of blend film. Among these nanofillers, nano-silica is commonly used in food packaging materials because it is one of FDA approved food additives (Peters et al., 2012) and it is also a low cost and biocompatible nanofiller. In order to improve the dispersion of nano-silica in the film, Yu, Li, Chu and Zhang (2018) developed a method for in situ nano-silica generation via hydrolysis of sodium metasilicate in the presence of PVA and CS acetic acid solution, which significantly improved the tensile strength of the PVA/CS blend film.

Liquefaction is a widely practiced biomass conversion method that is typically carried out under mild reaction conditions using acids as the catalyst and polyhydric alcohols as the solvent to destroy the chemical backbones to degrade the biomass and further functionalize the resulting fragments (Jasiukaitytė, Kunaver, & Strlič, 2009; Li et al., 2015; Pierson, Chen, Bobbink, Zhang, & Yan, 2014; Yamada & Ono, 2001; Yamada, Aratani, Kubo, & Ono, 2007; Zhang et al., 2006). In our previous research (Zhang et al., 2018; Zheng et al., 2019), we utilized the liquefaction method to convert commercial chitin and shrimp shells into liquified products, which showed good solubility in water and most organic solvents. The mechanism study indicated that depolymerization and deacetylation reactions occurred during the liquefaction process. The liquefied products were mingled with PVA to afford the blend films that exhibited good mechanical and thermal properties, water resistance, biodegradability and antibacterial activity. The manufactured blend films were believed to have potential applications for food packaging materials. However, their relevant properties in food packaging still remain a lot of room for improvement. In the present work, in situ generated silica reinforced PVA/LBMC (liquefied ball-milled chitin) blend films were prepared and their preliminary exploration as food packaging materials was carried out. Tensile strength and elongation tests were conducted to demonstrate the effect of silica on the mechanical properties of the PVA/LBMC blend film. Scanning electron microscopy (SEM), Fourier transform infrared spectroscopy (FTIR), X-ray powder diffraction (XRD) and thermogravimetric analysis (TGA) tests were carried out to characterize the morphology, structure and thermal properties. Moreover, the degradation properties of the blend films in soil and the fresh storage performance were evaluated for the purpose of biodegradable food packaging film.

2. Material and methods

2.1. Materials

Chitin from Zhejiang Gold-shell Biochemical Co., Ltd was dried at 105 °C for 12 h. The dried raw materials were ground thoroughly with a planetary ball mill, as described in our previous publication (Zhang et al., 2018). Polyethylene glycol 400 (PEG 400), glycol (Gl) and ethanol were purchased from Xilong Chemical Co., Ltd. Polyvinyl alcohol (PVA, 1750 ± 50, 99 % hydrolyzed) was purchased from Sinopharm Chemical Reagent Co., Ltd. $Na_2SiO_3{\cdot}9H_2O$ was purchased from Guangzhou Reagent Co., Ltd. All commercially available chemicals and reagents were of analytical grade or higher purity.

2.2. SiO_2 in situ reinforced PVA/LBMC blend films by hydrolysis of sodium metasilicate

The preparation of silica reinforced PVA/LBMC blend films are summarized schematically in Fig. 1. First, chitin (4.0 g) was liquefied by our previous reported method (Zhang et al., 2018) in a mix solvent of PEG 400 and Gl (28.0 g, 4:1, w/w) with H_2SO_4 (2.0 g) as catalyst to give LBMC. The hydroxyl number and average molecular weight of LBMC were measured to be 285 and 5145, respectively. Then PVA (20.0 g) was stirred in deionized water (480.0 g) at 90 °C to provide a 4 wt % of homogeneous solution. LBMC (0.5 g) was added into the PVA solution (50.0 g) and stirred at 65 °C for 3 h to afford a PVA/LBMC solution, in which the original mass ratio of chitin to PVA was calculated to be about 3 %. Thereafter, different concentrations (0, 0.1, 0.2, 0.4, 0.8 and 1.6 wt %) of Na_2SiO_3 aqueous solutions were slowly added to the PVA/LBMC solution, respectively, to achieve a series of uniform solutions. The Na_2SiO_3 would be hydrolyzed into SiO_2 in situ due to presence of sulfuric acid in the solution. Finally, the homogeneous solutions were individually poured onto clean glass plates and naturally dried at room temperature to give a series of blend films. The obtained films were

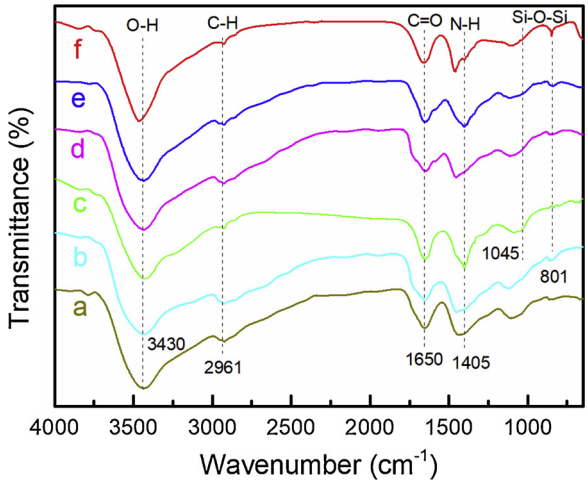

Fig. 2. FTIR spectra of blend films: (a) 4PVA-LBMC, (b) 4PVA-LBMC-0.1Si, (c) 4PVA-LBMC-0.2Si, (d) 4PVA-LBMC-0.4Si, (e) 4PVA-LBMC-0.8Si and (f) 4PVA-LBMC-1.6Si.

carefully kept in sealed bags for further analysis. The thickness of the film was measured as approximately 0.08 mm by vernier caliper. The PVA/LBMC films with 0, 0.1, 0.2, 0.4, 0.8 and 1.6 wt % of Na_2SiO_3 were designated as 4PVA-LBMC, 4PVA-LBMC-0.1Si, 4PVA-LBMC-0.2Si, 4PVA-LBMC-0.4Si, 4PVA-LBMC-0.8Si and 4PVA-LBMC-1.6Si, respectively.

2.3. Structure and morphology characterization

The FTIR spectroscopy of blend films were recorded on a Bruker TENSOR207 Fourier transform infrared spectrometer. All the test specimens were prepared by the regular KBr-disk method. The spectra were recorded in the frequency ranging from 4000 to 650 cm^{-1} with 32 scans. XRD spectra was conducted by a Bruker D8 X-ray diffractometer. The cross-section morphology of blend films was imaged at 10 kV using a Hitachi S3500 N scanning electron microscope. The films were rinsed with alcohol and gold sputtered prior to the SEM observation.

2.4. Mechanical property characterization

Tensile tests of the blend films were carried out on a WDW-1 universal testing machine at a speed rate of 50 mm/min. The specimens were cut into dumbbell shapes with length 75 mm and width 4 mm. Each sample was tested for five times and the average values and standard deviations were calculated.

2.5. Thermogravimetric analysis

Thermogravimetric analysis of films was performed on a NETZSCH5 209F3 thermogravimetric analyzer in a temperature range from 40 to 800 °C at a heating rate of 20 °C/min under N_2 atmosphere.

2.6. Measurements of browning index

The fresh cherries were washed by distilled water and randomly divided into five groups. The water on the surface was wiped off by filter paper. One group of cherries was the control group, without any packaging, while the other four groups were the experimental groups, wrapped in the blend films with different silica content. The weight loss and browning index of the cherries were calculated according to the literature method (Tian, Li, & Xu, 2005) after 7 days. Peel browning severity was divided into four levels: 1 = no browning; 2 = less than 1/4 browning; 3 = 1/4–1/2 browning; 4 = more than 1/2 browning. The browning index was calculated by the following Eq. (1), where N_i and N are the number of cherries at the browning level and the total number of cherries under treatment, respectively.

$$\text{Browning index} = \frac{\Sigma(\textit{browning level} \times N_i)}{N} \quad (1)$$

2.7. Biodegradability in the soil

Natural soil was filled in a 15 cm deep box. The blend films were buried to a depth of 10 cm from the soil surface for totally 30 days, which were taken out every 3 days, washed with deionized water, and dried at 65 °C (Park, Kim, Yoo, & Im, 2010). During the degradation period, water was supplied at a regular interval (Kim, Yoo, & Im, 2010). The weight loss of the blend films at different burial times was calculated to obtain the degradation curve. The degradation percentage was calculated by the following Eq. (2), where w and w_t are the initial weight and the dried weight at different buried days, respectively.

$$Is\,(\%) = \frac{W - W_t}{W} \times 100\% \quad (2)$$

3. Results and discussion

3.1. Structure characterization of blend films

With the gradual addition of Na_2SiO_3, the pH value of PVA-LBMC solution significantly raised (Fig. S1). When 0.2 wt % of Na_2SiO_3 was added, the pH value of the PVA-LBMC solution was near neutral by changing from 3.1 to 6.8. When the amount of Na_2SiO_3 added was higher than 0.2 wt %, the mixture presented as an alkaline solution. The pH value changes should be caused by the acid consuming hydrolysis of Na_2SiO_3 to SiO_2.

FTIR spectroscopy was used to investigate the structure of blend films. The FTIR spectra of 4PVA-LBMC films with different amount of Na_2SO_3 are displayed in Fig. 2. As shown, the broad and strong adsorption band at ~3430 cm^{-1} was designated to the overlapping stretching vibration absorption of the −OH and −N−H. Upon the addition of Na_2SiO_3, the absorption band was slighted narrowed and shifted to a higher wavenumber by ~10 cm^{-1}, indicating the partial broken of inter- and intra-molecular H-bonding of PVA and LBMC. The band at ~2961 cm^{-1} corresponded to the stretching vibration of $-CH_2$. The absorption at 1650 cm^{-1} (C=O stretching) and 1400–1450 cm^{-1} (N−H stretching) indicated the incomplete deacetylation of chitin in LBMC, which was consistent with our previous report (Zhang et al., 2018). After the addition of silica, the spectra of film showed new faint but not negligible peaks at 1045 cm^{-1} and 801 cm^{-1}, which were attributed to the Si−O−Si stretching vibration and the Si−O symmetric stretching (Tang, Xiong, Tang, & Peng, 2009; Xiong, Tang, Tang, & Zou, 2008). These results suggested SiO_2 was in situ synthesized under the acid condition introduced by LBMC.

The crystalline structure of PVA/LBMC blend films with various content of silica were investigated by XRD. As presented in Fig. S2, the 4PVA-LBMC film showed a main crystalline plane at about 2θ = 19.8° caused by the semi-crystalline character of PVA (Qiu, Liu, Jiang, & Chen, 2007; Zhang, Liu, Chen, & Chen, 2007). Moreover, the band intensity at 2θ = 19.8° slightly decreased with increasing Na_2SO_3 content, possibly because the silica formed in situ was easily dispersed into the polymer chain to form hydrogen bonds with PVA and LBMC. This interaction obstructed the ordered packing of PVA chains, leading to decreased crystallinity of the blend films (Qiang et al., 2009; Zheng et al., 2019). Although the decrease of crystallinity was not obvious, it still gave some hints that the addition of Na_2SiO_3 should have certain influence on the mechanical properties of the blend films.

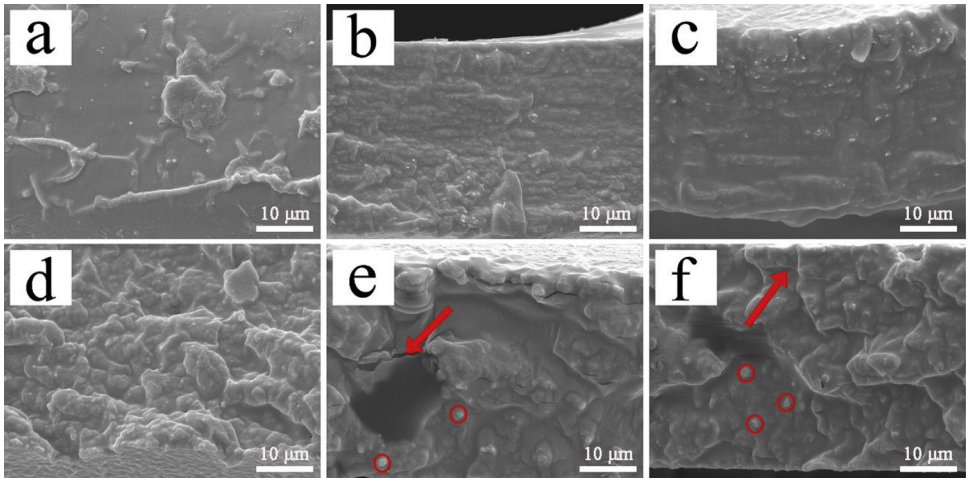

Fig. 3. The cross-section SEM images at 5.00 kx magnification of (a) 4PVA-LBMC, (b) 4PVA-LBMC-0.1Si, (c) 4PVA-LBMC-0.2Si, (d) 4PVA-LBMC-0.4Si, (e) 4PVA-LBMC-0.8Si and (f) 4PVA-LBMC-1.6Si.

3.2. Cross-section SEM images of the blend films

The morphology of the blend films was investigated by SEM. Fig. 3 displays the SEM images of cross-sectional morphology of 4PVA-LBMC blend films with various content of silica. A smooth sheet with micro-rods could be observed in the 4PVA-LBMC blend film (Fig. 3a), where the cross-linked LBMC and PVA were considered to form the large bulk sheets, and the remaining undisturbed LBMC was dispersed around the sheets. After the addition of Na_2SiO_3, united nano/micro-particles were presented and well dispersed in the blend films (Fig. 3b–d). However, when the Na_2SiO_3 content was higher than 0.4 wt %, nonnegligible cracks (red arrows) and obvious aggregates of nano-particles (red circles) appeared in the cross section of the blend films (Fig. 3e and f).

3.3. Mechanical properties of blend films

Tensile strength and elongation were measured to investigate the mechanical properties of blend films. As shown in Fig. 4, with the increase of silica content, the tensile strength of the blend films increased first and then decreased, while the elongation at break remained basically unchanged. When the content of Na_2SiO_3 was 0.2 wt % (4PVA-LBMC-0.2Si), the tensile strength and elongation reached the maximum values of 51 MPa and 994 %, an increase of 65 % and 2 %, respectively, compared to the 4PVA-LBMC blend film. The similar observations have been reported by previous researchers by using nano-silica as reinforcing agent (Ching, Rahman, Ching, Sukiman, & Cheng, 2015; Rane, Savadekar, Kadam, & Mhaske, 2014). This behavior should be attributed to the hydrogen bonds formed between SiO_2 and PVA/LBMC. Therefore, it could be concluded that the interaction between PVA/SiO_2 and LBMC/SiO_2 dominated the improvement of mechanical properties of the blend films. However, when the content of Na_2SiO_3 was higher than 0.2 wt %, SiO_2 formed in situ accumulated to form some defects, resulting in stress concentrations and brittleness of the blend films (Wang, Wei, Xia, Chen, & He, 2013). Fig. S3 shows the effect of the introduction of nano-silica on the Young's modulus of the blend films. A small amount of nano-silica led to an increase in the Young's modulus, which should be attributed to the inherent stiffness and rigidity of nano-silica that restricted the movement of PVA/LBMC macromolecules (Ching et al., 2015).

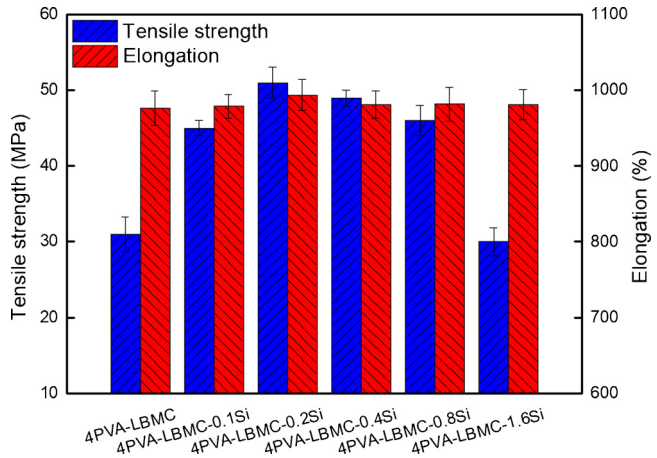

Fig. 4. Effect of Na_2SiO_3 content on the mechanical performance of the blend films.

3.4. Thermal properties of the blend films

The thermal stability of the blend films was studied by TGA and DTG analysis. Fig. 5a shows the TGA plots of the blend films with different silica content, which underwent three thermal degradation stages in the range of 60–500 ℃. The first stage was mainly the volatilization of water, residual solvents and oligomers at 60–180 ℃. The second stage might be the lateral decomposition of PVA and LBMC at 180–350 ℃. And the final stage was probably the breakdown of polymer molecular skeleton at a temperature range of 350–500 ℃ (Kuo, Sain, & Yan, 2014). It could be seen that the presence of silica was conducive to improving the thermal stability of the blend films in the second degradation stage, especially for the 4PVA-LBMC-0.2Si blend film. At this stage, its weight loss rate was 30 %, which was better than the 35 % weight loss rate of 4PVA-LBMC blend film without silica. Moreover, the DTG data shows that the temperature for the maximum weight loss rate (T_{DTGMAX}) of the 4PVA-LBMC-0.2Si film was 307 ℃, which was significantly higher than the 265 ℃ of the 4PVA-LBMC film (Fig. 5b and Table 1). The increased T_{DTGMAX} should be attributed to the hydrogen bonding force between SiO_2 and PVA and LBMC (Yu et al., 2018). In addition, the statistic heat-resistant index temperature (Ts) was calculated by Eq. (3). The data in Table 1 was recorded at temperatures of 5 % (T_5) and 30 % (T_{30}) weight loss rate.

$$T_s = 0.49\,(T_{d5} + 0.6\,(T_{d30}–T_{d5})) \quad (3)$$

3.5. Preservation tests

The preservation properties of the PVA/LBMC blend films were tested with fresh cherries, and the browning index was measured by

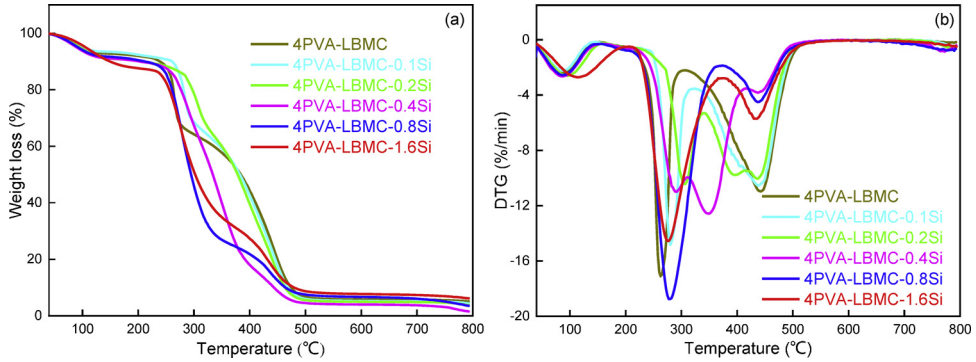

Fig. 5. (a) TGA curves and (b) DTG curves of the blend films.

Table 1
TGA data of the blend films.

Codes	T_{d5} (℃)	T_{d30} (℃)	T_s (℃)	T_{DTGMAX} (℃)	R_{800} (%)
4PVA-LBMC	98.3	270.3	98.7	264.5	5.12
4PVA-LBMC-0.1Si	101.3	294.3	106.4	282.4	4.29
4PVA-LBMC-0.2Si	95.6	315.8	111.6	306.8	3.68
4PVA-LBMC-0.4Si	89.5	295.0	104.3	291.0	1.50
4PVA-LBMC-0.8Si	92.2	273.0	98.3	279.0	3.41
4PVA-LBMC-0.16Si	102.6	268.2	99.0	275.5	6.06

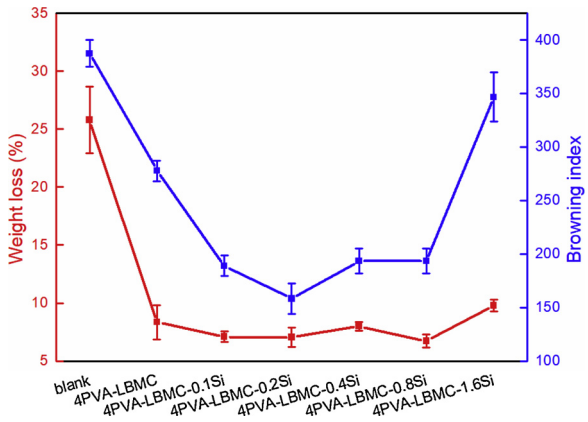

Fig. 6. The weight loss and browning index of cherries preserved by blend films after 7 days (blank: cherries exposed to the air under the same conditions).

recording the weight loss of film-packed cherries. As shown in Fig. 6, when the cherries were exposed directly to the air without a film packaging, the weight loss and browning index reached 26 % and 388, respectively. When coated with 4PVA-LBMC blend film, the weight loss obviously decreased to 8% and browning index decreased to 278. Surprisingly, when packed with silica involved blend film 4PVA-LBMC-0.2Si, these two data were further decreased, with the minimum values of 7 % and 158, respectively. The significant decrease of the browning index might be due to the tortuous path of gas permeation caused by the well-dispersed SiO_2 formed in situ, thereby enhancing the barrier to food spoiled gases. However, a further increase of Na_2SiO_3 content led to an increase of weight loss and browning index, which was probably due to the cracks in the blend films caused by the accumulation of silica, as characterized by SEM results. Thus, the 4PVA-LBMC-0.2Si blend film was identified to have the best preservation performance.

3.6. Biodegradability in the soil

The biodegradation behavior of selected blend films was characterized by soil burial. As shown in Fig. 7, the percentage of weight loss of the 4PVA-LBMC blend film was high to 52 % after 30 days of

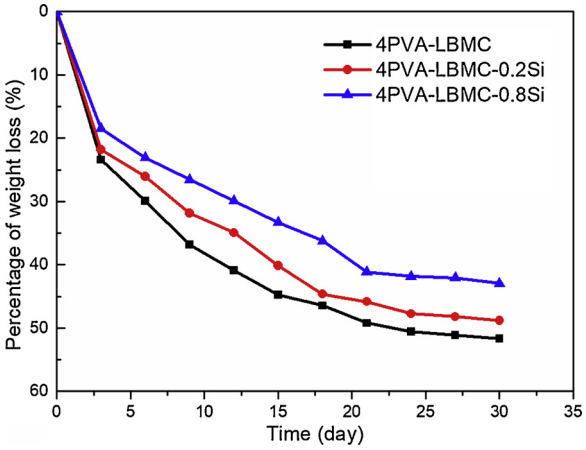

Fig. 7. Biodegradation of the blend films in the soil.

burial. After the incorporation of silica, the weight loss percentage was slightly reduced, but still maintained at a high level of biodegradation. It was speculated that the reduction in weight loss of the silica incorporating blend films was due to the formation of dense structure between silica and PVA/LBMC (Ismail & Zaaba, 2012), thereby delaying the dissolution time. Compared with traditional food packaging materials, the blend films can be rapidly degraded and quickly disappear itself in the soil owing to the dissolution.

4. Conclusion

A series of in situ generated silica reinforced PVA/LBMC blend films with 0–1.6 wt % Na_2SiO_3 were prepared by the hydrolysis of Na_2SiO_3. The FTIR result and pH value changes provided the evidences for the formation of silica after the addition of Na_2SiO_3. The SEM investigation suggested that the small amount of silica synthesized in situ could be well dispersed in the film. The optimized silica reinforced film was determined as 4PVA-LBMC-0.2Si, which showed the best mechanical property, thermal stability and preservation performance. In addition, the film also exhibited good degradability in the soil. Therefore, this in situ synthesized silica obviously improved the properties of PVA/LBMC blend films. The optimized blend film is considered to be a promising biodegradable material for food packaging.

CRediT authorship contribution statement

Jie Zhang: Investigation, Writing - original draft. **Wen-Rong Xu:** Conceptualization, Writing - review & editing. **Yu-Cang Zhang:** Resources, Project administration. **Xu-Dong Han:** Methodology. **Chen Chen:** Formal analysis. **Ao Chen:** Formal analysis.

Acknowledgments

We acknowledge the financial supports from the Natural Science Foundation of Hainan Province (No. 219QN258), the National Natural Science Foundation of China (No. 21978059, 51762013), the Health Institute Research Foundation (2019ZR03). We would like to thank the Analytical and Testing Center of Hainan University for the technical support and guidance.

Appendix A. Supplementary data

Supplementary material related to this article can be found, in the online version, at doi:https://doi.org/10.1016/j.carbpol.2020.116182.

References

Abdelgawad, A. M., Hudson, S. M., & Rojas, O. J. (2014). Antimicrobial wound dressing nanofiber mats from multicomponent (chitosan/silver-NPs/polyvinyl alcohol) systems. *Carbohydrate Polymers, 100*(100), 166–178.

Aider, M., Arul, J., Mateescu, A.-M., Brunet, S., & Bazinet, L. (2006). Electromigration of chitosan d-glucosamine and oligomers in dilute aqueous solutions. *Journal of Agricultural and Food Chemistry, 54*(17), 6352–6357.

Alminderej, F. M., & El-Ghoul, Y. (2019). Synthesis and study of a new biopolymer-based chitosan/hematoxylin grafted to cotton wound dressings. *Journal of Applied Polymer Science, 136*(1), 47625.

Aye, K. N., Karuppuswamy, R., Ahamed, T., & Stevens, W. F. (2006). Peripheral enzymatic deacetylation of chitin and reprecipitated chitin particles. *Bioresource Technology, 97*(4), 577–582.

Broek, L. A. M. V. D., Knoop, R. J. I., Kappen, F. H. J., & Boeriu, C. G. (2015). Chitosan films and blends for packaging material. *Carbohydrate Polymers, 116*, 237–242.

Ching, Y. C., Rahman, A., Ching, K. Y., Sukiman, N. L., & Cheng, H. C. (2015). Preparation and characterization of polyvinyl alcohol-based composite reinforced with nanocellulose and nanosilica. *BioRes, 10*(2), 3364–3377.

Felix, J. M., & Gatenholm, P. (2010). The nature of adhesion in composites of modified cellulose fibers and polypropylene. *Journal of Applied Polymer Science, 42*(3), 609–620.

Goy, R. C., Britto, D. D., & Assis, O. B. G. (2009). A review of the antimicrobial activity of chitosan. *Polímeros, 19*(3), 241–247.

He, M., Wang, X., Wang, Z., Chen, L., Lu, Y., Zhang, X., et al. (2017). Biocompatible and biodegradable bioplastics constructed from chitin via a “Green” pathway for bone repair. *ACS Sustainable Chemistry & Engineering, 5*(10), 9126–9135.

He, M., Wang, Z., Cao, Y., Zhao, Y., Duan, B., Chen, Y., et al. (2014). Construction of chitin/PVA composite hydrogels with jellyfish gel-like structure and their biocompatibility. *Biomacromolecules, 15*(9), 3358–3365.

Ifuku, S., Ikuta, A., Egusa, M., Kaminaka, H., Izawa, H., Morimoto, M., et al. (2013). Preparation of high-strength transparent chitosan film reinforced with surface-deacetylated chitin nanofibers. *Carbohydrate Polymers, 98*(1), 1198–1202.

Ismail, H., & Zaaba, N. F. (2012). The mechanical properties, water resistance and degradation behaviour of silica-filled sago starch/PVA plastic films. *Journal of Elastomers and Plastics, 46*(1), 96–109.

Jasiukaitytė, E., Kunaver, M., & Strlič, M. (2009). Cellulose liquefaction in acidified ethylene glycol. *Cellulose, 16*(3), 393–405.

Jayakumar, R., Prabaharan, M., Kumar, P. T. S., Nair, S. V., & Tamura, H. (2011). Biomaterials based on chitin and chitosan in wound dressing applications. *Biotechnology Advances, 29*(3), 322–337.

Kim, E. Y., Yoo, Y. T., & Im, S. S. (2010). Effect of hydrophilicity on the biodegradability of polyesteramides. *Journal of Applied Polymer Science, 90*(10), 2708–2714.

Kittle, J. D., Wang, C., Qian, C., Zhang, Y., Zhang, M., Roman, M., et al. (2012). Ultrathin chitin films for nanocomposites and biosensors. *Biomacromolecules, 13*(3), 714–718.

Koga, H., Nagashima, K., Huang, Y., Zhang, G., & Yanagida, T. (2019). Paper-based disposable molecular sensor constructed from oxide nanowires, cellulose nanofibers, and pencil-drawn electrodes. *ACS Applied Materials & Interfaces, 11*(16), 15044–15050.

Kumar, M. N. V. R., Muzzarelli, R. A. A., Muzzarelli, C., Sashiwa, H., & Domb, A. J. (2004). Chitosan chemistry and pharmaceutical perspectives. *Chemical Reviews, 104*(12), 6017–6084.

Kuo, P. Y., Sain, M., & Yan, N. (2014). Synthesis and characterization of an extractive-based bio-epoxy resin from beetle infested Pinus contorta bark. *Green Chemistry, 16*(7), 3483–3493.

Li, J., Xu, G., Luo, X., Xiong, J., Liu, Z., & Cai, W. (2018). Effect of nano-size of functionalized silica on overall performance of swelling-filling modified nafion membrane for direct methanol fuel cell application. *Applied Energy, 213*, 408–414.

Li, S. Q., Ni, H. G., & Zeng, H. (2017). PAHs in polystyrene food contact materials: An unintended consequence. *The Science of the Total Environment, 609*, 1126–1131.

Li, W., Zhang, Y., Li, J., Zhou, Y., Li, R., & Zhou, W. (2015). Characterization of cellulose from banana pseudo-stem by heterogeneous liquefaction. *Carbohydrate Polymers, 132*, 513–519.

Liu, B., Xu, H., Zhao, H., Liu, W., & Li, Y. (2017). Preparation and characterization of intelligent starch/PVA films for simultaneous colorimetric indication and antimicrobial activity for food packaging applications. *Carbohydrate Polymers, 157*, 842–849.

Mural, P. K. S., Kumar, B., Madras, G., & Bose, S. (2016). Chitosan immobilized porous polyolefin as sustainable and efficient antibacterial membranes. *ACS Sustainable Chemistry & Engineering, 4*(3), 862–870.

Park, C., Kim, E. Y., Yoo, Y. T., & Im, S. S. (2010). Effect of hydrophilicity on the biodegradability of polyesteramides. *Journal of Applied Polymer Science, 90*(10), 2708–2714.

Peelman, N., Ragaert, P., Meulenaer, B. D., Adons, D., Peeters, R., Cardon, L., et al. (2013). Application of bioplastics for food packaging. *Trends in Food Science & Technology, 32*(2), 128–141.

Peresin, M. S., Habibi, Y., Zoppe, J. O., Pawlak, J. J., & Rojas, O. J. (2010). Nanofiber composites of polyvinyl alcohol and cellulose nanocrystals: Manufacture and characterization. *Biomacromolecules, 11*(3), 674–681.

Peters, R., Kramer, E., Oomen, A. G., Herrera Rivera, Z. E., Oegema, G., Tromp, P. C., et al. (2012). Presence of nano-sized silica during in vitro digestion of foods containing silica as a food additive. *ACS Nano, 6*(3), 2441–2451.

Pierson, Y., Chen, X., Bobbink, F. D., Zhang, J., & Yan, N. (2014). Acid-catalyzed chitin liquefaction in ethylene glycol. *ACS Sustainable Chemistry & Engineering, 2*(8), 2081–2089.

Qiang, Z., Qian, J., An, Q., Zhu, M., Yin, M., & Sun, Z. (2009). Poly(vinyl alcohol)/polyelectrolyte complex blend membrane for pervaporation dehydration of isopropanol. *Journal of Membrane Science, 343*(1), 53–61.

Qiu, G. Z., Liu, Q. L., Jiang, Z. Y., & Chen, Y. (2007). Anti-trade-off in dehydration of ethanol by novel PVA/APTEOS hybrid membranes. *Journal of Membrane Science, 287*(2), 237–245.

Rabea, E., Badawy, M., Stevens, C., Smagghe, G., & Steurbaut, W. (2003). Chitosan as antimicrobial agent: Applications and mode of action. *Biomacromolecules, 4*, 1457–1465.

Rane, L., Savadekar, N., Kadam, P., & Mhaske, S. (2014). Preparation and characterization of K-carrageenan/nanosilica biocomposite film. *Journal of Materials, 2014*, 1–8.

Siripatrawan, U., & Noipha, S. (2012). Active film from chitosan incorporating green tea extract for shelf life extension of pork sausages. *Food Hydrocolloids, 27*(1), 102–108.

Song, W., Wei, W., Wang, D., & Zhang, S. (2017). Preparation and properties of new plywood composites made from surface modified veneers and polyvinyl chloride films. *Bioresources, 12*(4), 8320–8339.

Tang, H., Xiong, H., Tang, S., & Peng, Z. (2009). A starch-based biodegradable film modified by nano silicon dioxide. *Journal of Applied Polymer Science, 113*(1), 34–40.

Tang, H., Zhang, P. T., Ryan, S. J., Baker, S. M., Wiesmann, W. P., & Rogelj, S. (2010). Antibacterial action of a novel functionalized chitosan-arginine against gram-negative bacteria. *Acta Biomaterialia, 6*(7), 2562–2571.

Tian, S. P., Li, B. Q., & Xu, Y. (2005). Effects of O 2 and CO 2 concentrations on physiology and quality of litchi fruit in storage. *Food Chemistry, 91*(4), 659–663.

Tripathi, S., Mehrotra, G. K., & Dutta, P. K. (2009). Physicochemical and bioactivity of cross-linked chitosan-PVA film for food packaging applications. *International Journal of Biological Macromolecules, 45*(4), 372–376.

Vakili, M., Rafatullah, M., Salamatinia, B., Abdullah, A. Z., Ibrahim, M. H., Tan, K. B., et al. (2014). Application of chitosan and its derivatives as adsorbents for dye removal from water and wastewater: A review. *Carbohydrate Polymers, 113*, 115–130.

Wang, C., Wei, J., Xia, B., Chen, X., & He, B. (2013). Effect of nano-silica on the mechanical, thermal, and crystalline properties of poly(vinyl alcohol)/nano-silica films. *Journal of Applied Polymer Science, 128*(3), 1652–1658.

Wang, S. F., Shen, L., Tong, Y. J., Chen, L., Phang, I. Y., Lim, P. Q., et al. (2005). Biopolymer chitosan/montmorillonite nanocomposites: Preparation and characterization. *Polymer Degradation and Stability, 90*(1), 123–131.

Wang, Y., Li, J., & Li, B. (2016). Nature-inspired one-step green procedure for enhancing the antibacterial and antioxidant behavior of a chitin film: Controlled interfacial assembly of tannic acid onto a chitin film. *Journal of Agricultural and Food Chemistry, 64*(28), 5736–5741.

Xiong, H. G., Tang, S. W., Tang, H. L., & Zou, P. (2008). The structure and properties of a starch-based biodegradable film. *Carbohydrate Polymers, 71*(2), 263–268.

Xu, Y., Ren, X., & Hanna, M. A. (2010). Chitosan/clay nanocomposite film preparation and characterization. *Journal of Applied Polymer Science, 99*(4), 1684–1691.

Yamada, T., & Ono, H. (2001). Characterization of the products resulting from ethylene glycol liquefaction of cellulose. *Journal of Wood Science, 47*(6), 458–464.

Yamada, T., Aratani, M., Kubo, S., & Ono, H. (2007). Chemical analysis of the product in acid-catalyzed solvolysis of cellulose using polyethylene glycol and ethylene carbonate. *Journal of Wood Science, 53*(6), 487–493.

Yan, L., Li, P., Zhou, W., Wang, Z., Fan, X., Chen, M., et al. (2019). Shrimp shell-inspired antifouling chitin nanofibrous membrane for efficient oil/water emulsion separation with in situ removal of heavy metal ions. *ACS Sustainable Chemistry & Engineering, 7*(2), 2064–2072.

Yu, Z., Li, B., Chu, J., & Zhang, P. (2018). Silica in situ enhanced PVA/chitosan biodegradable films for food packages. *Carbohydrate Polymers, 184*, 214–220.

Zhang, J., Xu, W. R., Zhang, Y., Li, W., Hu, J., Zheng, F., et al. (2018). Liquefied chitin/polyvinyl alcohol based blend membranes: Preparation and characterization and antibacterial activity. *Carbohydrate Polymers, 180*, 175–181.

Zhang, Q. G., Liu, Q. L., Chen, Y., & Chen, J. H. (2007). Dehydration of isopropanol by novel poly(vinyl alcohol) – silicone hybrid membranes. *Industrial & Engineering Chemistry Research, 46*(3), 913–920.

Zhang, Y., Ikeda, A., Hori, N., Takemura, A., Ono, H., & Yamada, T. (2006). Characterization of liquefied product from cellulose with phenol in the presence of sulfuric acid. *Bioresource Technology, 97*(2), 313–321.

Zheng, F.-Y., Li, R., Hu, J., Zhang, J., Han, X., Wang, X., et al. (2019). Chitin and waste shrimp shells liquefaction and liquefied products/polyvinyl alcohol blend membranes. *Carbohydrate Polymers, 205*, 550–558.